

## Symmetry rules in magnetic core-level photoelectron spectroscopy from epitaxial ferromagnetic ultrathin films

R. Schellenberg,\* H. Meinert, A. Perez, and E. Kisker

*Institut für Angewandte Physik, Heinrich-Heine-Universität Düsseldorf, D-40225 Düsseldorf, Germany*

(Received 5 December 2000; published 23 August 2001)

For two x-ray incidence directions onto an epitaxial FeNi(001) film, one to the left and a second one to the right side of the symmetry plane spanned by the magnetization direction and the photoelectron wave vector, we have measured distributions of the emission-angle dependence with respect to the crystallographic axes of the Fe  $2p_{3/2}$  core-level photoelectron intensity asymmetry occurring upon magnetization reversal. The two angular distributions transform into each other when the signs of the magnetization and of the photoelectron emission angle are inverted, in accordance with the conservation of parity.

DOI: 10.1103/PhysRevB.64.104427

PACS number(s): 79.60.-i

### I. INTRODUCTION

Experimentally, one of the easiest methods to obtain information on element-specific local magnetic moments in heterogeneous materials is the exploitation of an asymmetry in the core-level photoelectron intensity occurring upon reversal of the sample magnetization. A conventional x-ray photoelectron spectrometer with a standard (unpolarized) soft x-ray source can be used,<sup>1</sup> upgraded to *remanently* magnetize the sample and to leave it in a magnetized state during the measurements without an applied external field. An intensity asymmetry of the order of 5% at  $\sim 0.8$ -eV total resolution occurs with unpolarized radiation, based on the existence of the so called magnetic linear dichroism in the angular distribution (MLDAD).<sup>2</sup> For the existence of such a dichroism with unpolarized or linear polarized radiation, the angular resolution of the photoelectrons is essential. Furthermore, the photoelectron wave vector, the magnetization, and the electric field vector must define a chirality, a right- or left-handed symmetry of these vectors.

The MLDAD has originally been explained on the basis of single-atom properties,<sup>3</sup> and it was indeed observed also in free, magnetically oriented atoms.<sup>4</sup> The parameters determining the MLDAD, which are accessible to external control, are the relative orientations of the light electric field vector ( $\mathbf{E}$ ), the magnetization ( $\mathbf{M}$ ), and the wave vector of the photoelectron ( $\mathbf{k}$ ). In the single-atom picture, the dichroism is proportional to the vector product<sup>5</sup>

$$D = \mathbf{E} \cdot (\mathbf{M} \times \mathbf{k})(\mathbf{k} \cdot \mathbf{E}). \quad (1)$$

Provided the geometric parameters are kept constant, the dichroism is thus proportional to the atomic magnetic moment. Element-specific magnetic properties of composite materials such as alloys<sup>6,7</sup> and ultrathin films<sup>8-15</sup> have been studied by that means.

In photoemission from single-crystalline samples, the propagation direction ( $\alpha$ ) of the photoelectrons with respect to the crystal axes affects the intensity due to photoelectron diffraction.<sup>16</sup> At photoelectron energies  $> 400$  eV, photoelectron diffraction results in pronounced forward-scattering peaks along the low-index crystallographic directions. It was observed that the photoelectron diffraction also has a strong

influence on the dichroism.<sup>5,17</sup> This is seen most clearly when the electron emission angle with respect to the crystal lattice ( $\alpha$ ) is varied by rotating the sample around the direction of  $\mathbf{M}$ . The external geometry determined by  $\mathbf{E}$ ,  $\mathbf{M}$ , and  $\mathbf{k}$  is thereby kept constant. In a single-atom picture, the dichroism should then be independent on  $\alpha$  since the latter is absent in Eq. (1). However, the experiment shows a significant dependence on the emission angle, i.e., a left-to-right-asymmetry pattern with respect to the forward-scattering peaks caused by photoelectron diffraction.<sup>18</sup> At normal emission, only the single-atom dichroism persists, which is smaller by about a factor of 3 than the asymmetry oscillations caused by photoelectron diffraction, the extreme values of which are occurring at emission angles of about  $\pm 6^\circ$ , respectively. Photoelectron-diffraction theory is able to explain the experimental data.<sup>18-20</sup> The dependencies of the dichroism on the relative directions of  $\mathbf{E}$  and  $\mathbf{k}$  [spanning the angle  $\Theta$ ] and  $\mathbf{E}$  and  $\mathbf{M}$  (spanning the angle  $\Phi$ ) have been studied in experiments on the Co  $3p$  core level by Kuch *et al.*<sup>21</sup> by varying the direction of  $\mathbf{E}$  keeping the electron emission direction normal to the surface. The  $\sin[2\Theta]$  dependence predicted by Eq. (1) was qualitatively confirmed. The dependence of the dichroism on the angle  $\Theta$  between  $\mathbf{E}$  and  $\mathbf{k}$ , keeping the absolute directions of  $\mathbf{E}$  and  $\mathbf{M}$  constant, has been studied by Hillebrecht *et al.*,<sup>5</sup> who observed a modulation of the atomic dichroism by photoelectron diffraction and electron escape-depth effects. The influence of the x-ray incidence angle on the *photoelectron-diffraction-related* dichroism, i.e., on the emission-angle dependence of the dichroism, has not been studied so far to our knowledge.

### II. EXPERIMENT

The subject of the present investigation is to compare dichroism data obtained subsequently taken on the same film in mirrorlike configurations, i.e., for x-ray incidence angles  $\pm \theta$ . The two incidence angles are realized by employing *two* x-ray sources, one mounted to the left and a second one mounted to the right side of the ( $\mathbf{M}, \mathbf{k}$ ) plane. The two geometries are approximately mirrorlike with respect to the plane.<sup>22</sup> We used the x-ray photoelectron spectrometer described earlier,<sup>20</sup> which enables us to measure the emission-angle dependence of the core-level energy distributions from

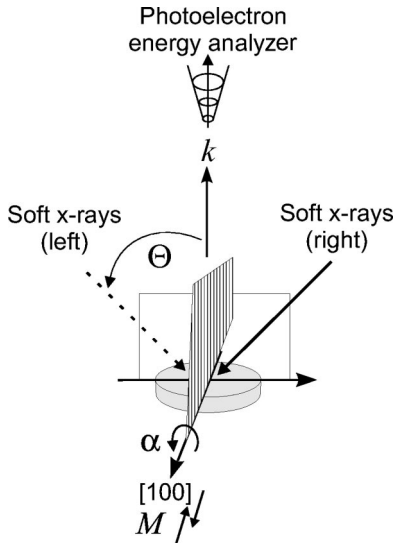


FIG. 1. The photoemission geometry. Unpolarized Mg  $K\alpha$  radiation is incident onto the sample either from the left or from the right side with respect to the mirror plane spanned by the magnetization direction and the acceptance direction of the photoelectron spectrometer. The rotation axis of the sample coincides with the magnetization direction.

remanently magnetized samples. The magnetization direction can be switched “up” or “down” by applying a small magnetic-field pulse, which is generated by a current pulse through a coil placed close to the sample. The sample can be rotated around an axis defined by the magnetization direction  $\mathbf{M}$  (see Fig. 1). Since the acceptance direction of the photoelectron spectrometer is fixed in space, the detected photoelectrons have traveled along different directions through the single crystal. We define the emission angle ( $\alpha$ ) as the angle between  $\mathbf{k}$  and the  $[001]$  direction of the crystal lattice in the  $(100)$  plane. For each emission angle ( $\alpha$ ), two energy distribution curves (EDC’s) are taken for the opposite magnetization directions to determine the binding energy ( $E_B$ ) dependence of the intensity asymmetry (“dichroism”). We will display the normalized intensity difference  $D = (I^\uparrow - I^\downarrow) / \max(I^\uparrow + I^\downarrow)$  for the two antiparallel magnetization directions as a measure of the dichroism, after subtraction of a constant background intensity given by the intensity at the high binding-energy side of the core-level peaks. By  $\max(I^\uparrow + I^\downarrow)$  we mean the maximum intensity value of the two summed EDC’s. The angle ( $\alpha$ ) is stepped computer controlled over a large range, thereby sweeping the sample’s surface normal across the entrance aperture of the electron spectrometer to obtain the  $D(E_B, \alpha)$  distributions. The sample was one epitaxial ultrathin film of  $\text{Ni}_{54}\text{Fe}_{46}$ , grown *in situ* in an ultrahigh vacuum on a  $\text{Cu}(001)$  substrate.

### III. RESULTS AND DISCUSSION

Figure 2 shows the intensity distribution curves of the Fe  $2p_{3/2}$  core-level as a function of the binding energy and of the emission angle. Photoelectron-diffraction peaks due to forward scattering are observed at normal emission ( $100^\circ$ ) and at a  $\pm 20^\circ$  emission angle, corresponding to emission along

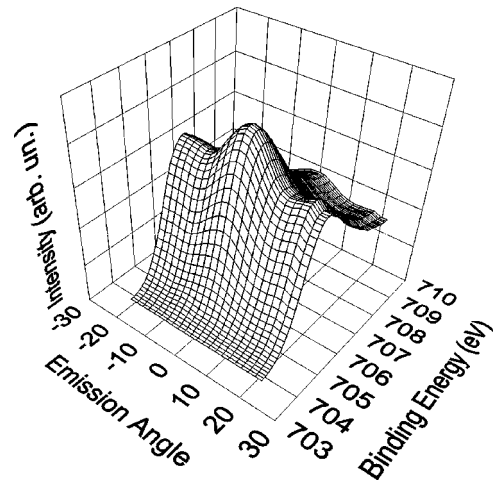


FIG. 2. The Fe  $2p_{3/2}$  intensity as a function of emission angle and binding energy.

the  $(112)$  direction. In the angular range covered in Fig. 2, the intensity distribution does not depend significantly on the specific x-ray source (left or right one). At larger angles, however, the angular distributions become different because of shadowing of the x-ray sources by part of the sample holder.

Figure 3 shows the binding-energy dependence of the dichroism at normal emission, obtained with the left and with the right x-ray sources. The main difference between the two curves is their opposite sign. It has been shown previously that at normal emission, photoelectron diffraction effects are absent and that the dichroism is determined by the atomic properties.<sup>20</sup> The opposite sign obtained for the two magnetization directions is in accordance with Eq. (1), i.e., changing  $+\theta$  to  $-\theta$  results in the opposite sign. This opposite sign of the dichroism in *normal* emission for x-ray incidence angles of  $\pm 45^\circ$  has been observed earlier by Kuch *et al.*<sup>21</sup> for the similar case of the Co  $3p$  core-level. Figure 4 shows the angular dependence of the photoemission intensity and of the dichroism obtained with both x-ray sources from the same magnetic film that had been used with the other x-ray source. With the right source, grazing incidence is approached near  $\alpha = 30^\circ$ , resulting in the intensity cutoff. The angular oscillation of the dichroism [cf. Fig. 4(b)] is known to be due to photoelectron diffraction.<sup>20</sup> The central question of this paper is the nature of the relationship between the two dichroism curves.

A more complete picture of the dichroism is obtained when the angular and binding-energy dependencies are combined in a single figure. This is shown in Fig. 5 and Fig. 6. The major features in these figures are the occurrence of one main peak or dip, which occurs either at a negative ( $\alpha = -6^\circ$ ) or a positive emission angle ( $+6^\circ$ ), depending on the x-ray source used. The peak (dip) in Fig. 5 and Fig. 6 obviously corresponds to the main peak (dip) at  $\alpha = -6^\circ$  ( $+6^\circ$ ) in Fig. 4(b). The graphs of the full data sets shown in Figs. 5 and 6 suggest that the dichroism patterns obtained with the left and right x-ray sources correspond to each other when both the angle and the asymmetry axes are reversed, rather than by rigidly shifting one of the patterns, as one

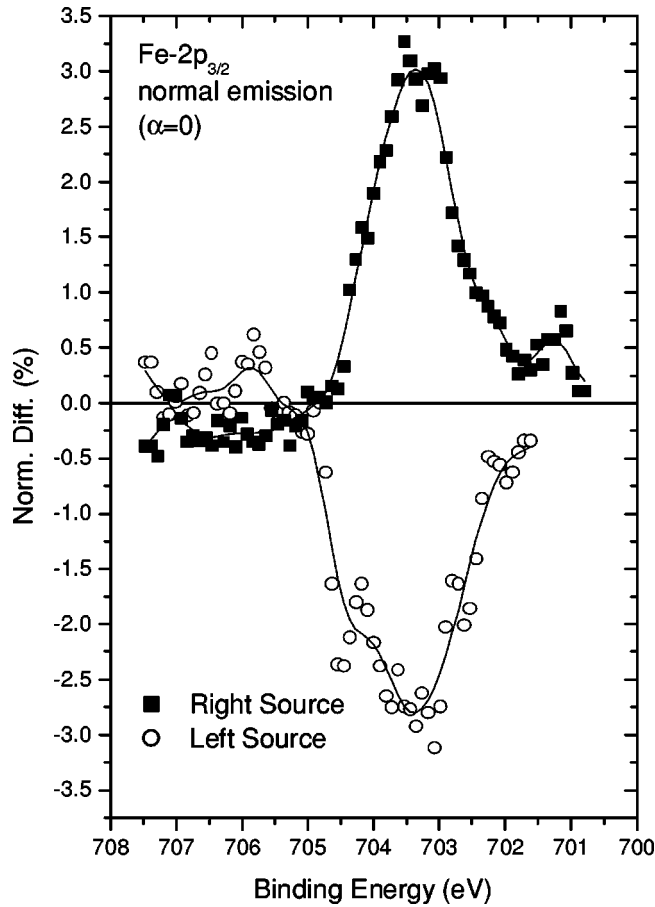


FIG. 3. The dichroism (intensity difference) of the Fe  $2p_{3/2}$  core level as obtained with the left and with the right x-ray sources, at normal emission.

might assume originally by inspection of Fig. 4(b) alone.

To interpret these observations, it is realized that the configuration {x-ray incidence left  $\cup \mathbf{M}^\uparrow$ } is obtained by mirroring the {x-ray incidence right  $\cup \mathbf{M}^\uparrow$ } configuration at the plane spanned by the magnetization direction and the photoelectron wave vector (cf. Fig. 1), taking into account the axial nature of the magnetization vector. In the mirror image, the rotation angle  $\alpha$  changes to  $-\alpha$ . Parity conservation implies that the experiment and its simple mirror image yield the same results.<sup>23</sup> Accordingly, our experimental results must be the same in the original and in the mirrored configuration.<sup>24</sup> As a test, we apply the mirror transformation  $\{\mathbf{M}^\uparrow \rightarrow \mathbf{M}^\downarrow, \alpha \rightarrow -\alpha\}$  to one of the angular dependencies that have been shown in Fig. 4. In Fig. 7 we compare the transformed angular dependence obtained with the right source, overlaid onto the angular dependence as obtained with the left source, after scaling to the same maximum height. The angular dependencies agree quite well. Small deviations might be explained by aging of the sample since the measurements are taken in sequence. This coincidence shows that in spite of their different appearance the two asymmetry distributions shown in Figs. 5 and 6 actually represent the same physical situation.

The  $D(E_B, \alpha)$  distributions for other core-levels and materials do not generally differ as drastically for  $+\theta$  and  $-\theta$  as

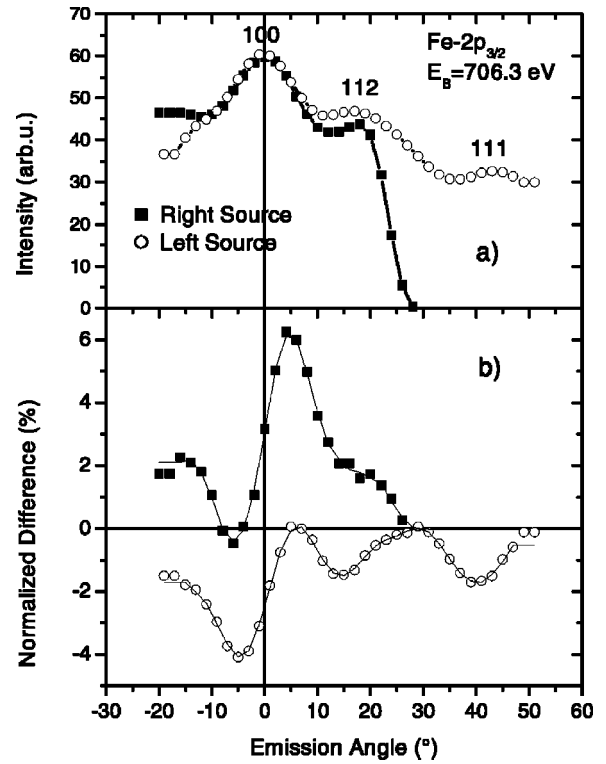


FIG. 4. The dependence of the photoelectron intensity (a) and of the dichroism (b) on the photoelectron emission angle with respect to the crystallographic axes. The binding energy has been set to the dichroism maximum according to Fig. 3

for the present case, shown in Figs. 5 and 6. As an example, we mention that the Fe  $3p$  core-level dichroism distributions (not shown here) for these two angles of x-ray incidence are virtually the same, being antisymmetric with respect to  $\alpha = 0$ , similar as in the case of Fe/Ag(100).<sup>20</sup> The antisymmetry is just an alternative expression of the transformation ( $\mathbf{M} \rightarrow -\mathbf{M}, \alpha \rightarrow -\alpha$ ). Hence also the  $3p$  distributions transform into each other by this symmetry rule.

Albeit an additional measurement with the second source, i.e., in the mirrored configuration, in principle does not give new physical information, it is advantageous in the following cases: First, the dichroism can also be determined without

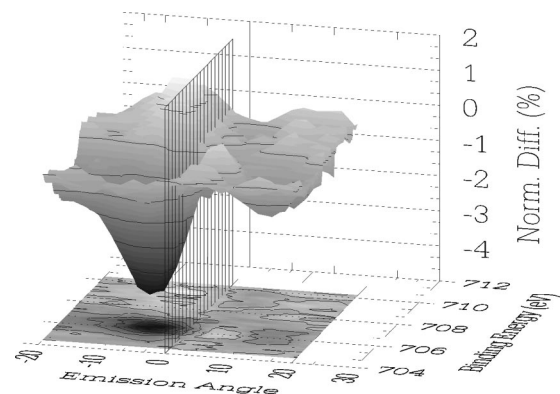


FIG. 5. The dichroism as a function of the binding energy and of the emission angle for x-ray incidence from the left side (cf. Fig. 1).

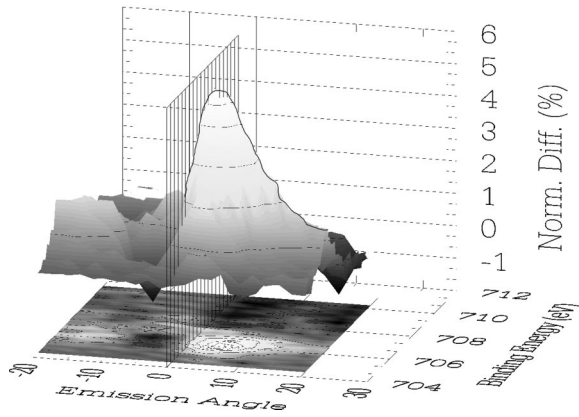


FIG. 6. The same as in Fig. 5, but with x-ray incidence from the right side.

flipping the sample magnetization or, alternatively, without rotating the sample azimuthally by  $180^\circ$ , since mirroring of the incident radiation direction is equivalent to inversion of the magnetization direction and, simultaneously (for off-normal emission), rotating the sample from  $-\alpha$  to  $+\alpha$  (cf. Fig. 1). Accordingly, the MLDAD in remanently magnetized samples with large coercive fields can be determined by using two radiation sources as an alternative to the methods described above. Furthermore, a potential instrumental asymmetry arising from the magnetization pulses can be determined and eliminated by comparing data obtained with both sources. If the intensity were systematically larger, e.g., for  $M^\uparrow$  than for  $M^\downarrow$ , one might conclude the existence of a dichroism. However, a dichroism changes sign when switching from  $+\theta$  to  $-\theta$  whereas an instrumental asymmetry due to a deflection of the electron beam by magnetic stray fields will not. Thus, this instrumental effect can be recognized by making use of those two x-ray sources. It is possible to restrict to normal emission ( $\alpha=0$ ). However, if the sample is rotated from  $\alpha=-6^\circ$  to  $\alpha=6^\circ$ , about a three times larger magnetic contrast as compared to normal emission is obtained (see Figs. 5 and 6). This results in about a 10 times larger “figure of merit” ( $A^2 \cdot I$ ) as compared to an experiment that uses normal emission only.

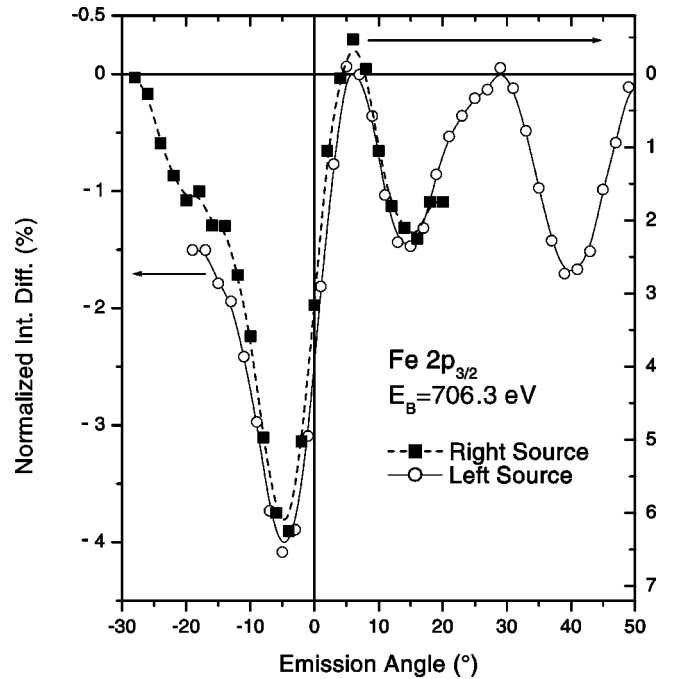


FIG. 7. Comparison of the angular distributions of the dichroism when unpolarized soft x rays are incident either from the left or from the right side with respect to the mirror plane as defined in Fig. 1, after application of the transformation  $\{M^\uparrow \rightarrow M^\downarrow, \alpha \rightarrow -\alpha\}$  and normalization to the same peak heights.

#### IV. CONCLUSIONS

We have shown that for mirrored x-ray incidence directions, the emission-angle dependencies of the photoelectron-diffraction-originated magnetic linear dichroism from a single-crystalline ferromagnetic sample transform into each other by substituting ( $M \rightarrow -M, \alpha \rightarrow -\alpha$ ), as expected from parity conservation.

#### ACKNOWLEDGMENTS

We thank F.U. Hillebrecht for helpful discussions. This work was supported by the Deutsche Forschungsgemeinschaft and by special grants from the Ministerium für Schule, Weiterbildung, Wissenschaft and Forschung Nordrhein-Westfalen.

\*Present address: Vacuumschmelze GmbH, Hanau, Germany.

<sup>1</sup>F.U. Hillebrecht and W.-D. Herberg, Z. Phys. B: Condens. Matter **93**, 299 (1994).

<sup>2</sup>C. Roth, F.U. Hillebrecht, H.B. Rose, and E. Kisker, Phys. Rev. Lett. **70**, 3479 (1993).

<sup>3</sup>N.A. Cherepkov, Phys. Rev. B **50**, 13 813 (1994).

<sup>4</sup>A. von dem Borne, T. Dohrmann, A. Verweyen, B. Sonntag, K. Godehusen, and P. Zimmermann, Phys. Rev. Lett. **78**, 4019 (1997).

<sup>5</sup>F.U. Hillebrecht, H.B. Rose, T. Kinoshita, Y.U. Idzerda, G. van der Laan, R. Denecke, and L. Ley, Phys. Rev. Lett. **75**, 2883 (1995).

<sup>6</sup>F.O. Schumann, R.F. Willis, K.G. Goodman, and J.G. Tobin, Phys. Rev. Lett. **79**, 5166 (1997).

<sup>7</sup>R. Schellenberg, E. Kisker, M. Faust, A. Fanelso, and F.U. Hillebrecht, Phys. Rev. B **58**, 81 (1998).

<sup>8</sup>G. Panaccione, F. Sirotti, E. Narducci, N.A. Cherepkov, and G. Rossi, Surf. Sci. **377**, 445 (1997).

<sup>9</sup>G. Panaccione, F. Sirotti, E. Narducci, and G. Rossi, Phys. Rev. B **55**, 389 (1997).

<sup>10</sup>G. Panaccione, P. Torelli, G. Rossi, G. van der Laan, M. Sacchi, and F. Sirotti, Phys. Rev. B **58**, R5916 (1998).

<sup>11</sup>X.Y. Gao, M. Salvietti, W. Kuch, C.M. Schneider, and J. Kirschner, Phys. Rev. B **58**, 15 426 (1998).

<sup>12</sup>W.A.A. Macedo, F. Sirotti, G. Panaccione, A. Schatz, W. Keune, W.N. Rodrigues, and G. Rossi, Phys. Rev. B **58**, 11 534 (1998).

<sup>13</sup>W.A.A. Macedo, F. Sirotti, A. Schatz, D. Guarisco, G. Panaccione, and G. Rossi, J. Magn. Magn. Mater. **177–181**, 1262 (1998).

- <sup>14</sup>M. Liberati, G. Panaccione, F. Sirotti, P. Prieto, and G. Rossi, Phys. Rev. B **59**, 4201 (1999).
- <sup>15</sup>G. Panaccione, P. Torelli, G. Rossi, G. van der Laan, P. Prieto, and F. Sirotti, J. Phys.: Condens. Matter **11**, 3431 (1999).
- <sup>16</sup>C.S. Fadley, Prog. Surf. Sci. **16**, 275 (1984).
- <sup>17</sup>A. Fanelsa, R. Schellenberg, F.U. Hillebrecht, and E. Kisker, Solid State Commun. **96**, 291 (1995).
- <sup>18</sup>A. Fanelsa, R. Schellenberg, F.U. Hillebrecht, E. Kisker, J.G. Menchero, A.P. Kaduwela, C.S. Fadley, and M.A. Van Hove, Phys. Rev. B **54**, 17 962 (1996).
- <sup>19</sup>H.B. Rose, T. Kinoshita, C. Roth, F.U. Hillebrecht, and E. Kisker, Surf. Rev. Lett. **4**, 915 (1997).
- <sup>20</sup>R. Schellenberg, E. Kisker, A. Fanelsa, F.U. Hillebrecht, J.G. Menchero, A.P. Kaduwela, C.S. Fadley, and M.A. Van Hove, Phys. Rev. B **57**, 14 310 (1998).
- <sup>21</sup>W. Kuch, M.-T. Lin, W. Steinhogel, C.M. Schneider, D. Venus, and J. Kirschner, Phys. Rev. B **51**, 609 (1995).
- <sup>22</sup>The incidence direction of the left source deviates from the mirrored incidence direction of the right source by a  $15^\circ$  tilt out of the incidence plane defined by the right source. The component of the electric vector parallel to  $M$ , which is present in this case, does not contribute to the dichroism according to Eq. (1). The result is a reduction of the dichroism obtained with the left source by 7% as compared to that expected for the exact mirror image of the right source.
- <sup>23</sup>J. Kessler, *Polarized Electrons* (Springer-Verlag, Berlin, 1976).
- <sup>24</sup>Violation of parity conservation in atomic electromagnetic interactions is very weak and can only be observed in *precision* experiments which are not within the scope of the present investigation. For a recent discussion on parity nonconservation in atomic physics, see S.C. Bennett and C.E. Wieman, Phys. Rev. Lett. **82**, 2484 (1999).